Zweitveröffentlichung/
Secondary Publication

Georg R. Pesch, Fei Du, Udo Schwientek, Caspar Gehrmeyer, Alexander Maurer, Jorg Thöming,
Michael Baune

Recovery of submicron particles using high-throughput dielectrophoretically switchable filtration

Recommended Citation (primary publication/Version of Record) incl. DOI:

Georg R. Pesch, Fei Du, Udo Schwientek, Caspar Gehrmeyer, Alexander Maurer, Jorg Thöming, Michael Baune,
Recovery of submicron particles using high-throughput dielectrophoretically switchable filtration,
Separation and Purification Technology, Volume 132, 2014, Pages 728-735, ISSN 1383-5866,
https://doi.org/10.1016/j.seppur.2014.06.028.

Take down policy

Recovery of submicron particles using high-throughput dielectrophoretically switchable filtration

Georg R. Pesch *, Fei Du, Udo Schwientek, Caspar Gehrmeyer, Alexander Maurer, Jorg Thöming, Michael Baune

Center for Environmental Research and Sustainable Technology (UFT), Department of Recovery and Recycling (VdW), University of Bremen, Leobener Str., 28359 Bremen, Germany

ABSTRACT

Conventional methods for separation of submicron particles, e.g., filtration or centrifugation, suffer from severe problems, such as loss of particles during resuspension and high energy demands due to fouling of separating membranes. Here we present the novel concept of dielectrophoretically switchable filtration using pore sizes that are two to three orders of magnitude larger than the particles. We used layer-by-layer (LbL) assembled nanocapsules of 340 nm diameter that were to be separated and recovered from polyelectrolyte solution. The filter being an insulating porous structure is placed in between two electrodes generating an electric field which is bend at the solid–liquid interface and is thus highly inhomogeneous. Dielectrophoresis (DEP) is used as a driving force to trap particles in the filter. The filtration is based on electric effects and could thus be easily turned off by switching off the electric field allowing safe and easy resuspension of the trapped nanocapsules. A parametric study has been conducted to investigate the influence of voltage, pore size, flux and membrane thickness on the separation efficiency. Maximum separation and recovery efficiencies in a semi-continuous run reached almost 65% when working with a specific flow rate of $4.12 \, \text{mL} \, \text{s}^{-1} \, \text{m}^{-2}$, a voltage of 200 V, frequency of 210 kHz and a filter with thickness of 1.5 mm and pore sizes in the range of 20–60 μm. The results demonstrate that electrically switchable retardation of nanoparticles is possible even in large flow systems. This finding paves the way for preparative DEP chromatography of nanoparticles. Its ease makes this switchable filtration attractive for nanoparticle separation and purification in general.

1. Introduction

The separation of charged particles in the nanometer range from a suspending fluid is challenging, especially if large quantities of particles have to be recovered from liquids containing polyelectrolytes of identical charge. While the throughput of centrifugation is limited and costly, membrane filtration techniques such as ultrafiltration (UF) and microfiltration (MF) suffer from severe fouling problems. This is especially true if a complete separation is required as in the case of colloidal multilayer systems. These systems have gained more and more attention over the past decade as they offer the possibility to produce tailor-made capsules combining different materials. Especially the feasibility to remove a solid core from a multilayer shell opened new prospects in biomedical applications [1–4]. Drugs can be protected in a smart and stable multilayer shell, which protects them from external influences until they reach the desired part in the human body [5,6] where they are triggered to open by a certain stimuli and release the drug [7–9]. They can be produced by a variety of mechanisms from which the layer-by-layer (LbL) [10] approach is the most promising due to its simplicity and broad range of practicability.

The buildup of LbL particles is driven by electrostatic forces between oppositely charged molecules: A charged substrate is immersed into a solution of polyions with opposite charge. Because of the attracting forces between the substrate charges and the polyions they adsorb onto the substrate surface and form a layer [10]. The substrate is then taken out of the first solution and is subsequently immersed into a second solution with polyions of charges which are again opposite to the surface charges of the substrate. This procedure may be repeated until the desired amount of layers has build up. Consecutive washing steps between the adsorption steps are necessary to avoid contamination of the solutions [10].

Separation of the solution and the substrate can be cumbersome when working with colloidal particles, especially if they are in the nanometer range [11]. Centrifugation [11], membrane filtration [12] and sequential adsorption [11] methods have

* Corresponding author. Tel.: +49 (0)421 213 63386; fax: +49 (0)421 218 9863386.
E-mail address: gpesch@uni-bremen.de (G.R. Pesch).

been developed 15 years ago and are still state-of-the-art although they suffer form severe problems [12,13]. Application of all three methods can lead to particle agglomeration and subsequent destruction of multilayer shells during re-dispersion [12]. In case of membrane filtration the formation of a filter cake leads to high particle loss and membrane fouling [12]. This could be avoided by keeping the particles suspended at all time; however, this is only achievable when working with a very low flow rate and through-put [12]. When centrifugation is used to separate the nanoparticles one has to work with low centrifugation velocities in order to avoid agglomeration. This makes the process very time intensive as several long centrifugation steps are required [12].

An approach to reduce fouling in membrane filtration processes is the superposition of electric fields. In Electrofiltration a stationary dc field produces an electrophoretic force on charged particles so that they levitate on top of the membrane instead of forming a filter cake. It has been successfully applied in cross-flow [14–18] and dead-end [19–21] filtration processes with continuously applied and pulsed [19,22] electric fields. Apart from the electrophoretic force, which is acting on the particles, an electroosmotic force is acting on the fluid and is intensifying the fluid flow through the membrane [23,22]. The electroosmotic effect could also be used as a driving force for membrane backwashing in order to remove deposited particles when the polarization of the electrodes is reversed [24]. To keep uncharged particles from depositing on the membrane the dielectrophoretic effect (DEP) could be used.

In DEP charged and uncharged particles are polarized in an inhomogeneous electric field. Depending on the properties of the liquid and the particles and on the electrode design a resulting DEP force either points towards or away from high electric field regions. Du et al. [25,26] and Molla et al. [27–29] have successfully shown that DEP could be used to reduce fouling in cross-flow membrane filtration processes.

Here, in contrast, we use a different approach and introduce a novel method to separate LbL assembled nanocapsules by superimposing an ac electric field to a dead-end filtration process. The concept of insulator-based DEP (iDEP) [30–35] is applied by introducing an insulating porous structure in between two electrodes for generating very high local electric field gradients. DEP is used as a driving force to move particles towards the pores surface where they are captured and filtered out of the solution. As the main separation mechanism is DEP controlled reversible trapping of the particles on sharp edges inside the filter, the pore size can be several times larger than the particle diameter.

Because particles are trapped mainly inside the pores the formation of a filter cake can be prevented. Since the separation of particles is based on electrical effects, the filter could be easily "switched off" by shutting down the electric field. This opens the possibility to easily recover the trapped particles by backwashing. Whereas DEP is used in anti-fouling concepts to move particles away from the membrane in a conventional filtration process, in our concept the DEP force points towards the solid material and is acting as the driving force for the filtration.

1.1. Theoretical background

Dielectrophoresis was firstly described by Pohl [36] as the translational movement of uncharged matter, e.g. particles, in non-uniform ac or dc electric fields. A particle located in an electric field experiences a dielectric polarization expressed as double-layer deformation of charged particles or charge redistribution in neutral particles [37]. It can be described as two equal but opposing charges which are unequally distributed on the particles surface, thus resulting in a macroscopic dipole [38]. If the superimposed electric field is non-uniform the field strength at both sides of the particle is different resulting in a net dielectrophoretical force. For a spherical particle with radius r located in a medium with given permittivity ε_M, the dielectrophoretic force in an ac field can be described by the dipole approximation [37,39]:

$$\boldsymbol{F}_{\text{DEP}} = 4\pi r^3 \varepsilon_0 \varepsilon_M \text{re}[K](\boldsymbol{E} \cdot \nabla)\boldsymbol{E} \tag{1}$$

with $\varepsilon_0 = 8.854 \cdot 10^{-12} \text{ F m}^{-1}$ being the permittivity of free space, E the intensity of the electric field, and re[K] the real part of the Clausius–Mossotti factor K, which defines the effective dielectric polarizability of the particle in a given medium. K is a function of the frequency f and depends on the dielectric properties of the particle and the medium [39]:

$$\text{re}[K] = \text{re}\left[\frac{\tilde{\varepsilon}_P - \tilde{\varepsilon}_M}{\tilde{\varepsilon}_P + 2\tilde{\varepsilon}_M}\right], \tag{2}$$

$$\tilde{\varepsilon} = \varepsilon - \frac{j\sigma}{\omega}. \tag{3}$$

Here, $\tilde{\varepsilon}$ is the complex permittivity of the particle or the medium (subscripts P and M, respectively), a quantity describing the polarizability of a material in ac fields [25], σ the conductivity, $\omega = 2\pi f$ the angular frequency of the applied electric field and $j = \sqrt{-1}$ the imaginary unit.

Balancing the dielectrophoretic and the viscous drag force yields the steady-state velocity of a spherical particle suspended in an aqueous solution [39]:

$$\boldsymbol{v} = \frac{2r^2 \varepsilon_0 \varepsilon_M \text{re}[K](\boldsymbol{E} \cdot \nabla)\boldsymbol{E}}{3\eta_M} \tag{4}$$

with the dynamic viscosity of the medium η_M. Eq. (4) is only valid if the medium is static or if the particles motion is independent of the fluid motion [39]. As Eqs. (1)–(4) show, the strength of the dielectrophoretic force and velocity is highly dependent on the particle radius (r^3 in Eq. (1) and r^2 in Eq. (4)), the difference in dielectric properties in combination with the frequency (Eqs. (2) and (3)), and the spatial change of the electric field (($\boldsymbol{E} \cdot \nabla)\boldsymbol{E}$). The direction of the DEP force is dependent upon the difference in polarizability of particles and medium which is expressed by re[K]. If the polarizability of the medium is lower than that of the particle, the DEP force will direct towards higher electric field regions (positive DEP), whereas, if the polarizability of the medium is higher than that of the particle, the force will direct towards lower electric field regions (negative DEP). The conductivity of a particle is not only defined by its bulk conductivity but also largely influenced by the double layer or surface conductance. The influence of the surface conductivity on the overall conductivity of the particle is increasing with decreasing particle size [40].

In microsystems usually bare electrodes are used, however, as with increasing applied voltage this might produce problems in aqueous solutions, such as corrosion of the electrode material, short circuits, and human electrical shock, an electric insulation on one or both electrodes may be mandatory [39]. In that case a high-pass filter is formed by the combination of insulated electrodes and liquid. It limits the DEP application in low-frequency regions and increases the overall energy requirement [39]. As a second side effect, DEP systems are usually superimposed by inevitable electrothermal effects (ETE), which may influence the particle movement. In general two electrothermal effects occur due to Joule heating: the electrothermal fluid flow, caused by local conductivity and permittivity changes due to the temperature gradient, and buoyancy, which is caused by local density differences. In systems with a characteristic dimension above 1 mm the Joule heating induced buoyancy always dominates the fluid flow [41]. It drives the fluid flow from high electric field regions towards areas with lower electric field, thus disturbing the DEP motion.

1.2. Proposed DEP filtration concept

Up to today, DEP has been developed and applied in trapping, separating, and handling of particles mainly in the biomedical industry in microfluidic systems usually at low flow rates and low throughputs [31,34,37,42–49]. To scale up the system for achieving higher volume flows (and thus throughput) usually the electrode distance has to be enlarged. As it can be seen from Eq. (4) the DEP velocity is dependent on the square of the electric field gradient and the square of the particle size. Enlarging the electrode distance at constant voltages the gradient of the electric field will be decreased and the field will become too weak to move small particles. Application of a higher voltage is, however, inevitably linked to higher energy demands and thus cost. Furthermore, a high electrode potential leads to a dramatic temperature rise of the fluid due to Joule heating in a confined system.

In the present paper we circumvent those scale-up problems by combining a deep-bed filtration process with the DEP effect. The conventional deep-bed filtration process is altered so that the filter, a dielectric with open porosity, is placed in between two electrodes which are connected to an ac voltage source. Due different dielectric properties, i.e., permittivity and conductivity, between the filter and the liquid medium the field lines are bent at the solid–liquid-interface. Hence, because of the inhomogeneity of the pore structure a non-uniform electric field is generated with local maxima of the electric field strength at the interface. The LbL produced nanocapsules have a higher polarizability at frequencies in the kHz range than the surrounding medium, an effect which can be attributed to the very high surface charge of the particles which is a consequence of the production mechanism, consisting of sequential adsorption of polyions on the particle surface. Subsequently, the particles have much higher surface charge compared to standard particles, such as latex spheres. Hence, they will experience a positive DEP effect at these frequencies. Therefore, they will be driven towards the pore surface and trapped while flowing through the filter. Particles that exhibit negative DEP force should be driven towards the center of the channel as the permittivity of the medium is much higher than that of the filter, resulting in much lower electric field strength in the liquid domain [50]. If no electric field is applied (Fig. 1a), particles flow through the porous structure as there is barely any mechanical filtration effect due to the big size difference between pores and particles. With a sufficient electric field applied (Fig. 1b), the DEP effect directs most of the particles towards the surface of the pores, where they reside until the field is turned off. This has mainly two advantages. Firstly, the formation of a filter cake is avoided, which not only generates a more stable permeate flux over time but also prevents the high particle loss during resuspension. Secondly, the filtration effect could be easily turned off, i.e., particles that are trapped in the filter could be safely resuspended by backwashing with water. The DEP velocity is highly influenced by $(\boldsymbol{E} \cdot \nabla)\boldsymbol{E}$ (Eq. (4)). This results in higher traveling velocities and thus better trapping of particles with increasing difference in the electric field strength (and thus also higher gradients in areas near the interface), i.e., with increasing difference in polarizability between filter and liquid medium [50].

2. Experimental section

A schematic overview of the setup used in this experiments is given in Fig. 2.

Two separation cells (1) with different dimensions were used. The parametric study for particle separation has been carried out using a square separation cell with an effective filter area of 1500 mm^2 (setup 1). Afterwards the setup was enlarged so that
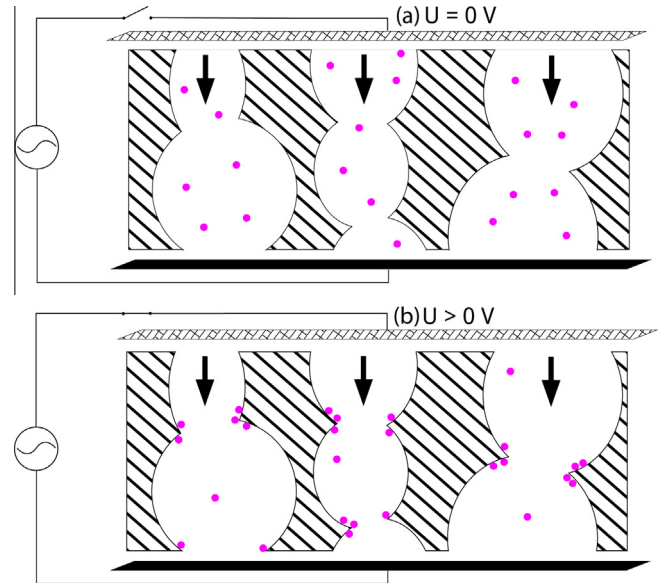

Fig. 1. Proposed mechanism of DEP intensified deed-bed filtration. A conventional deep-bed filtration unit is altered, so that the filter is placed in between of two electrodes. (a) If the electric field is turned off, particles that are much smaller than the pore size simply flow through the filter. (b) If sufficient voltage is applied, particles are directed by a DEP force towards the surface of the pores.
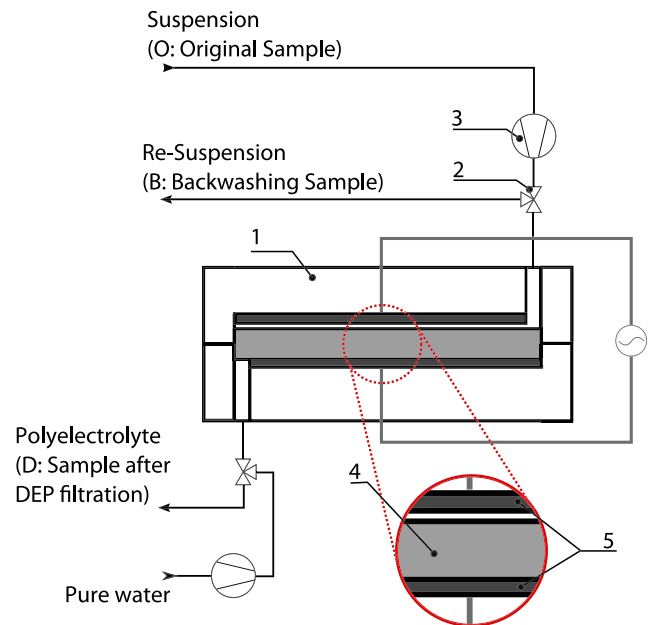

Fig. 2. Schematic overview of the DEP intensified deep-bed filtration unit. 1: separation cell; 2: valve; 3: syringe pump; 4: filter; and 5: electrode.

the volume flow could be increased with constant separation efficiency. The setup for the backwashing experiments and the semi-continuous test run had an effective filter area of 4050 mm^2 (setup 2). The separation cell consisted of two parts which were screwed together.

The filters (4) used for the experiments (Manufacturer: DIA-Nielsen GmbH & Co. KG) were made of polyethylene (PE) with an irregular pore structure and different mean pore diameters. Two different electrodes (5) where used to generate the electric field. On the inlet side a rolled extruded titan metal grid with a mesh size of 9.4 mm^2 was used. A V2A stainless steel plate was used on the outlet side. Both electrodes were manufactured by the workshop

3

of the University of Bremen. The distance between the two electrodes was 20 mm. Both electrodes were assembled into clearances in the acrylic glass cell. The mesh of the grid electrode was filled with an epoxi-compound. The electrodes were connected to the ac voltage source by isolated screw fittings. The ac signal provided by a VOLTCRAFT 7202 function generator was amplified by an FM 1290 amplifier (FM Elektronik Berlin). All experiments were conducted using a sinus input signal with a frequency of 210 kHz. The grid electrode in the setup was isolated by polypropylene (PP), which was glued onto the metal grid. Special care had to be taken to avoid air bubbles between the metal grid and the insulation material. Fluid inlet and outlet were realized by using Swagelog adapters. A syringe pump (3) KDS-100-CE (kdScientific) was used for inputting suspension. The nanoparticle suspension for the experiments was provided by Surflay Nanotec. The nanocapsules are pink in color with a mean diameter of 340 nm and a narrow size distribution (measured with a Malvern ZetaMaster S) and concentration of 0.1 wt% in the colorless polyelectrolyte PSS ($1 \, g \, L^{-1}$) in 0.2 M NaCl, 10 mM NaAc buffer (pH 5.6). They were made of silica particles covered in a shell of rhodamin labeled poly(allylamine hydrochloride). Surface charge of the colloids was negative. Preliminary experiments have been conducted using simple interdigitated electrodes to test the particles DEP behavior. A picture of the electrodes used (Netzsch IDEX Sensor Heads 065S) for this setup is shown in Fig. 3a. They consisted of nickel which was applied on a polyimide support. The polarization of these electrodes is shown in Fig. 3b. Distance of the electrodes was $d_1 = 115 \, \mu m$ with the electrodes being $d_2 = 100 \, \mu m$ wide. The electrode was placed in an acrylic glass chamber with a 5 mm slit on top of the electrode. After inputting the nanocapsule solution, the electric field was turned on with a variety of voltages and frequencies in and below the kHz range. Particle motion was observed with a 30 fps black and white camera (Sony XCD-X710). Particles always displayed positive DEP motion in their polyelectrolyte, as they were moved and trapped to the edge of the electrode fingers, where the electric field strength is maximum [51].

UV/Vis spectrophotometry (CADAS 200, Dr. Lange) was used to quantify the separation efficiency. A calibration curve was obtained at a wavelength of 560 nm, which is the adsorption peak of the nanocapsules, by diluting the original input suspension, which consists of the polyelectrolyte solvent and the nanocapsules, with pure polyelectrolyte solution in different concentrations from compositions with 10 vol% pure polyelectrolyte (pure polyelectrolyte means polyelectrolyte without any nanocapsules) and 90 vol% original nanoparticle suspension to compositions with 90 vol% pure polyelectrolyte. The calibration curve gives a linear dependence between the composition of the mixture (and thus nanoparticle concentration) and adsorption at 560 nm. Adsorption was measured before each experiment to find the concentration of the input suspension. The separation efficiency was defined as $1 - (c_{out}/c_{in})$, which is the ratio of the output concentration c_{out} and the input concentration c_{in} of the purified original suspension.

Each experiment from the parametric study was conducted 3 times. Diagrams show the average value with the error bars representing the standard deviation.

In backwashing experiments, in order to purify the nanocapsules from the electrolyte after each separation experiment, air was pressed through the setup with the electric field turned on for removing all excess polyelectrolyte. By keeping the electric field on, trapped particles stay inside the system. The recovery efficiency for backwashing experiments is defined as the amount of recovered particles obtained by measuring the output concentration divided by the ostensible amount of particles in the filter from the preceding experiments, a value easily calculated with the separation efficiency and the input suspension concentration.

3. Results and discussion

By using a grid electrode the electric field distribution without the porous dielectric between the electrodes is already inhomogeneous, which could be considered as the global inhomogeneity of the electric field. By introducing the filter in between the electrodes, the field is further disturbed and local inhomogeneities arise. Inhomogeneities on the global scale, however, are rather small and negligible for the movement of particles. Nevertheless, as the field is already disturbed, the local inhomogeneities tend to be stronger; some preliminary studies showed, that the separation efficiency is always higher when working with a grid as top electrode compared to working with a plate as top electrode.

Fig. 4 shows three typical samples of a DEP filtration experiment. Sample O is the original input suspension, as obtained by the supplier. Sample B is the backwashing sample as obtained by recovery experiments (cf. Section 3.2). Sample D is taken after DEP filtration experiments. The change in turbidity is obvious: Sample O is very turbid, which is caused by the nanocapsules. Sample D is almost transparent, indicating that most of the particles are retarded in the filtration process as the pure polyelectrolyte is
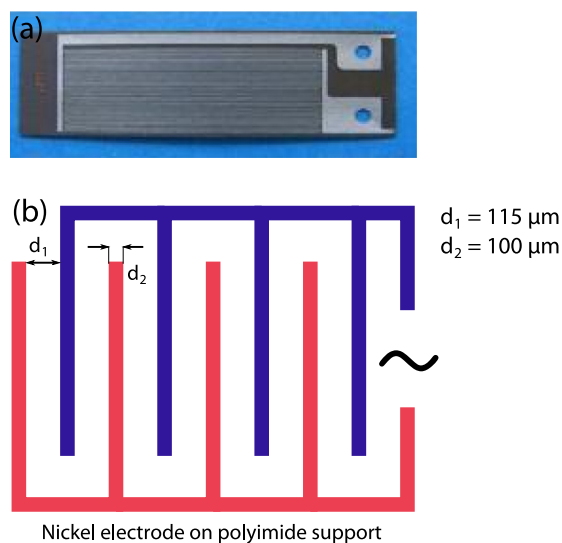

Fig. 3. (a) Electrodes used for testing particles DEP behavior in preliminary experiments (Netzsch IDEX-Sensor Head 065S). (b) Polarization and geometry of electrodes. Interdigitated electrodes are finger like structures which are sequentially oppositely polarized. The distance between two fingers was $d_1 = 115 \, \mu m$ and each finger is $d_2 = 100 \, \mu m$ wide.

Fig. 4. Typical samples after filtration experiments. O: Original Sample, B: Backwashing Sample, and D: Sample after DEP filtration.

4

colorless. Sample B is less turbid than O, which is caused by the fact that the nanocapsule concentration is much lower (cf. Section 3.2).

3.1. Separation efficiency

Fig. 5 shows the separation efficiency as a function of the pore size for 1 mm thick PE filters with a feed flow rate of $Q = 30$ mL h^{-1} which equals 5.56 mL s^{-1} m^{-2}. Separation efficiencies are compared for processes without and with a superimposed electric field with a frequency f of 210 kHz and voltage $U = 200$ V. As expected, due to the much larger pore size ($d > 20$ μm) than particle diameter (340 nm), only a marginal quantity of the particles is retarded by the filter without superimposed electric field. The separation efficiency increases from $1.9 \pm 2.7\%$ to $7.0 \pm 0.4\%$ with a decrease of pore size from 130 μm to 20 μm. This is because of the higher adsorption of nanocapsules onto the pore surface and could thus be referred to as mechanical filtration efficiency.

The strength of the local electrical field gradient is highly influenced by the material and the structure of the porous media. It will be increased with the inhomogeneity of the structure, i.e., with smaller pores. Then, the DEP induced velocity of nanocapsules should increase with decreasing pore size. If an electric field is superimposed, the filtration efficiency is increasing from $19.5 \pm 4.4\%$ to $31.6 \pm 2.9\%$ for the three investigated filters. Firstly, this can be attributed to the fact that, with smaller pore size, higher inhomogeneities of the electric field are induced, thus leading to higher DEP forces and velocities. Secondly, smaller pore sizes lead to shorter travel distances for the particles to be captured. Consequently both, the mechanical and the DEP trapping efficiency is increased, when a fine-pored filter (pore size $d = 20$–60 μm) is used. A fine-pored filter, however, is linked to a higher pressure loss and thus higher operational costs as compared to a coarse-pored (pore size $d = 80$–130 μm) filter.

The residence time of the particles inside the filter could be increased by decreasing the flow rate Q. With a constant separation cell size, the velocity of the medium and the particle through the filter is increasing with increasing flow rate. This leads to a shorter residence time of the particles inside the filter and hence shorter motion distance towards the pore surface. A higher residence time allows particles to travel larger distances towards the surface of the pore during their stay in the filter. Subsequently separation efficiency is decreasing with volume flow because particles need to reach the pore surface to achieve separation. Therefore, if the residence time is too short, no effective separation is possible, as shown in Fig. 6. This is also supporting the assumption that DEP is one of the main trapping mechanisms inside the filter as a
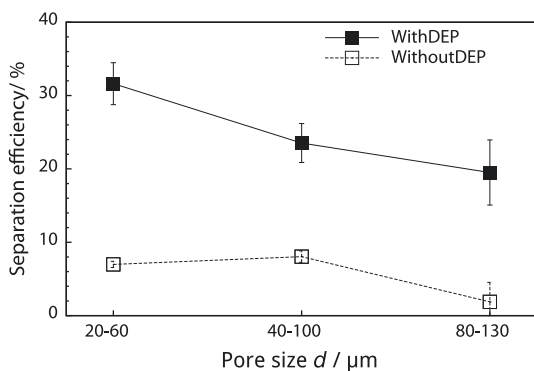

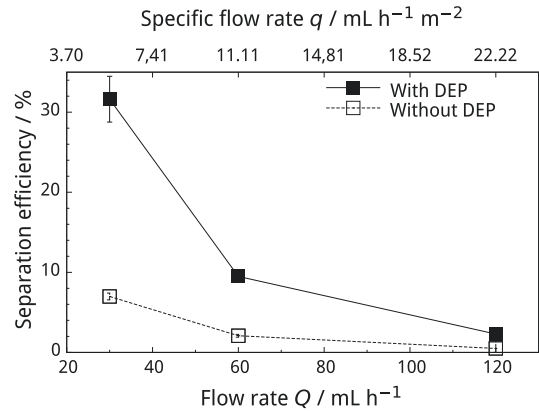**Fig. 6.** Separation efficiency as a function of the feed flow rate Q. Frequency of the applied electrical field $f = 210$ kHz and voltage $U = 200$ V. PE filter with a pore size of $d = 20$–60 μm and thickness $h = 1$ mm.

separation due to size exclusion would be independent of the flow rate and filter thickness.

Again, if the electric field is turned off, almost no separation can be achieved when working with a $h = 1$ mm thick PE filter with pore sizes between $d = 20$–60 μm. Then, the separation efficiency is gradually increasing from $0.5 \pm 1.8\%$ to $7.0 \pm 0.4\%$ with a decrease of Q from 120 mL h^{-1} to 30 mL h^{-1}. If the electric field is turned on ($U = 200$ V), the separation efficiency is significantly higher at low flowrate. With increasing volume flow it is rapidly decreasing from up to $31.6 \pm 2.9\%$ at $Q = 30$ mL h^{-1} to $2.3 \pm 0.5\%$ at $Q = 120$ mL h^{-1}.

Another option to increase residence time of particles is to increase their pathlength, i.e., by increasing the filter thickness. This in turn would increase the separation efficiency, as shown in Fig. 7. This effect was experimentally validated for filters with three different pore sizes and thicknesses. There is almost no difference in separation efficiency for a filter with 1 mm thickness for the three investigated pore sizes. Additionally, filters with pore sizes from 40–130 μm show almost the same separation efficiency which is only slightly increasing with filter thickness from $h = 1.5$ mm to $h = 2$ mm. A significant difference is observable for filters with pore sizes $d = 20$–60 μm, with the separation efficiency increasing from 26.7 ± 2.5 at $d = 1.5$ mm to 36.4 ± 1.9 at $d = 2$ mm. The results demonstrate that the effect of increasing separation is the strongest for the finest of the three filters. We assume this is because the mechanical trapping efficiency is much larger for filter with smaller pore size. Mechanical trapping efficiency is then also heavily influenced by the filter thickness leading to the high separation efficiency for the fine-pored filter shown in Fig. 5.

Due to the quadratic dependence of the applied voltage on the DEP velocity (Eq. (4)), the separation efficiency is highly influenced by the voltage as presented in Fig. 8. With the applied electric field, the separation efficiency under the stated conditions (flow rate $Q = 60$ mL h^{-1}, frequency $f = 210$ kHz, filter pore size $d = 80$–160 μm, filter thickness $h = 1$ mm) reached almost 20% when a voltage of $U = 200$ V is applied. The separation efficiency decreases with decreasing U in a more than linear manner until it is similar to that without electrical field at $U = 160$ V. A higher DEP velocity increases the chance of particles to reach the pore walls during their residence time inside the filter. This means, if the DEP velocity of the particles is too low to be trapped during the residence time, they will simply travel through the filter. Hence, separation efficiency is highly dependent on the voltage of the applied electric field, as indicated by Fig. 8. Furthermore, the DEP effect is not sufficient to effectively trap the nanocapsules in the filter if working with $U < 200$ V.

Fig. 5. Separation efficiency as a function of filter pore size d. Flow rate $Q = 30$ mL h^{-1}, frequency $f = 210$ kHz, voltage $U = 200$ V. PE filter thickness $h = 1$ mm.
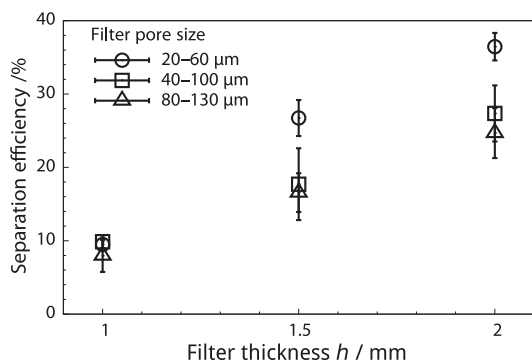
Fig. 7. Separation efficiency of DEP filter as a function of filter thickness h for three different pore sizes. Frequency of the applied electrical field $f = 210$ kHz and voltage $U = 200$ V. Flow rate $Q = 60$ mL h^{-1}.
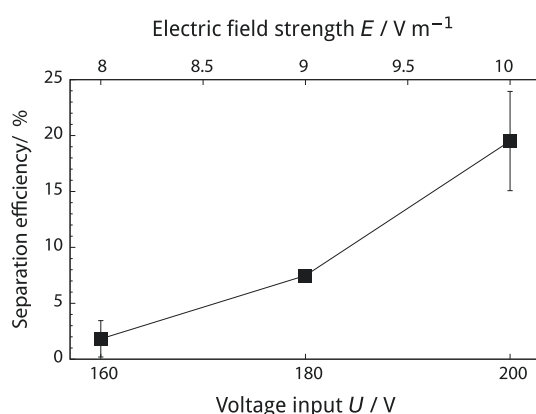

Fig. 8. Separation efficiency as a function of applied voltage U. Flow rate $Q = 30$ mL h^{-1}, frequency $f = 210$ kHz. PE filter with pore size $d = 80$–160 μm and thickness $h = 1$ mm.

Filters with pore sizes from 80–160 μm and flow rates of $Q = 60$ mL h^{-1} have been used in Figs. 6 and 7 because, as already discussed, small pores lead to higher pressure loss and thus operational cost and low flow rates decrease the throughput. Our goal is, however, to investigate the feasibility of a high-throughput operation at low cost, thus we chose those parameters as a trade-off.

To summarize shortly, we showed that the superposition of ac electric fields is dramatically increasing the separation efficiency of 340 nm nanocapsules in filters with pore sizes from $d = 20$–130 μm. Separation efficiency without electric field are in the range of 0–8% and are increasing with superimposed electric field to values up to 36% with ideal flow and electric field parameters. Separation efficiency (both, DEP and non-DEP separation efficiency) is increasing with filter thickness, decreasing pore size, and decreasing flux. DEP separation efficiency is increasing with voltage.

3.2. Semi-continuous process for particle recovery

One of the main advantages of DEP enhanced deep-bed filtration is the possibility to easily recover the nanocapsules after separation. For these experiments we used a filtration module of more than twice the size of the one used for the separation efficiency parametric study presented before (see Section 2, setup 2). The setup was enlarged to achieve higher throughputs with constant separation efficiency. As expected separation efficiency at constant flow rate increased clearly. Up to almost 65% were achieved

(cf. Fig. 9). A recovery flow rate of at least $Q_{bw} = 180$ mL h^{-1} was found to be necessary to effectively resuspend trapped particles. In the present work backwashing is conducted with pure water at a flow rate of $Q_{bw} = 360$ mL h^{-1} after the setup has been flushed with air several times.

Fig. 9 shows the recovery efficiency as a function of the achieved separation efficiency when working with a recovery flow rate of $Q_{bw} = 360$ mL h^{-1}.

All three experiments were obtained with the same separation and filter parameters (separation flow rate $Q = 60$ mL h^{-1} and filter pore size $d = 20$–80 μm). The filter used for the experiments of the present paper do not have a uniform pore size distribution. Thus, although working with the exact same parameters for nanocapsule trapping, different separation efficiencies were achieved. This influences the recovery efficiency; we assume that filters which where used when a high separation efficiency has been achieved have an overall finer pore structure. This in turn leads to a lower recovery efficiency as the overall backwashing volume flow through larger pores is much higher due to the lower flow resistance, making particle recovery easier from larger pores.

As indicated in Fig. 9, recovery efficiencies are in the order of 40%–60% when working with the stated parameters. For calculating the recovery efficiency it was assumed that the loss of trapped particles in the filtration module during draining is negligible. The recovery efficiency seems to be highly influenced by the history of the filter (e.g., temperature during filtration, separation efficiency and filtration time) and long-term experiments, as described as follows, are required to better understand the parameter influence on the recovery efficiency.

For investigating semi-continuous operation mode the bigger filtration module was used (see Section 2, setup 2). For this system higher separation efficiencies were obtained even with a high separation flow rate of $Q = 60$ mL h^{-1} and a recovery flow rate of $Q_{bw} = 360$ mL h^{-1}. The applied voltage was $U = 200$ V with a frequency of $f = 210$ kHz. A PE filter with pore size $d = 20$–60 μm and thickness $h = 1.5$ mm was used.

After 15 min separation procedure, nanocapsules were recovered with the electric field turned off for a duration of 2 min. In each step, two 5 mL samples were taken and measured. The average of separation efficiency and recovery efficiency from taken samples is shown in Fig. 10. The trend lines for both separation and recovery efficiency, as presented in Fig. 10, indicate that a steady separation efficiency can be reached in a certain time. The recovery efficiency increases with time. On the one hand, the accumulation of trapped particles in the filter over time is obviously increasing the recovery efficiency. On the other hand, the like nanocapsules have identical surface charges resulting in repelling electrostatic interparticle forces. These forces are weaker than
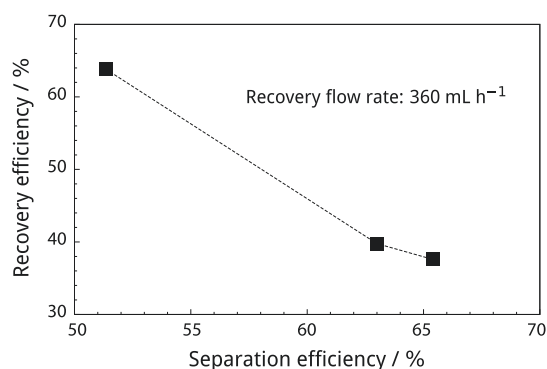

Fig. 9. Recovery efficiency of trapped nanocapsules as a function of separation efficiency. Recovery flow rate $Q_{bw} = 360$ mL h^{-1}.
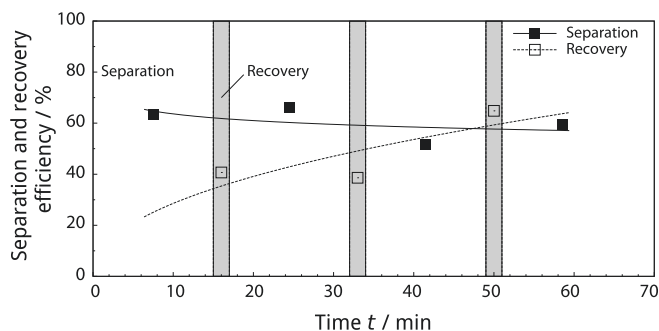
Fig. 10. Semi-continuous test run for nanocapsule separation and recovery for a duration of 60 min. Separation has been conducted with a flow rate of $Q = 60$ mL h^{-1} for a duration of 15 min and two subsequent samples have been taken at the end from which the mean values are presented. Recovery steps have been conducted with a flow rate of $Q = 360$ mL h^{-1} for a duration of 2 min. Two samples have been taken from which the mean values are shown. Filtration was performed with a 1.5 mm PE filter with pore size $d = 20–60\ \mu$m. Parameters of the electric field: $U = 200$ V and $f = 210$ kHz.

the DEP force—however, with the electric field switched off this leads to an automatic resuspending of those particles, which are not trapped directly on the filter material but on other trapped particles.

The decrease of the separation efficiency over the course of the process from 63% at $t = 7.5$ min to 52% at $t = 41.5$ min can mainly be attributed to the accumulation of trapped nanocapsules inside the filter from previous steps, which could not be removed effectively during the backwashing step (recovery efficiency is only 41% at $t = 16$ min and 39% at $t = 33$ min). This might not directly influence the separation efficiency as the same amount of particles is trapped even when there is already a large amount of trapped particles in the filter from the preceding steps; however, already trapped particles might be resuspended during the course of separation and washed out together with the purified polyelectrolyte solution. This might cause the small decrease in separation efficiency over time.

Fig. 11 gives an overview of possible trapping and resuspending mechanisms. Fig. 11A shows the trapping of nanocapsules with the electrical field turned on. Particles can move through the filter without reaching areas in which they are trapped (trajectory (a)). If they are close enough to the surface or if they travel through small pores they will reach the surface of the pores during the residence
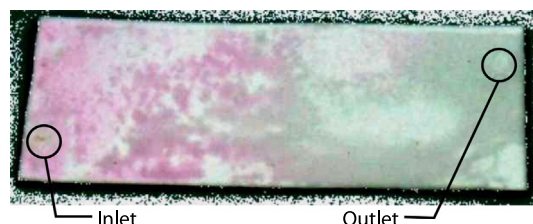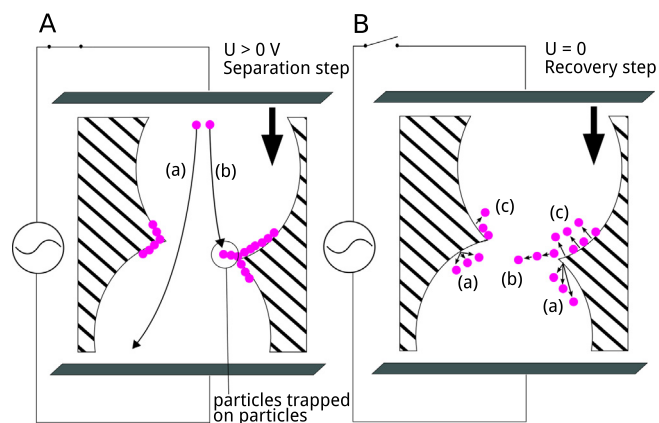

Fig. 11. DEP deep-bed filtration. (A) Trapping of nanocapsules in the DEP deep bed filtration. (a) Trajectory of particle passing the filter without reaching the pores surface. (b) Trajectory of particle which is trapped in the filter. Particles could be trapped on other particles as indicated by the circle. (B) Resuspension of particles. For description of (a), (b) and (c) in part B, see text.

Fig. 12. A typical filter (setup 2) after filtration experiments. Pink colored areas mark the region of the filter where most of the particles have been separated. Fluid is unequally distributed at areas close the inlet before crossing the filter, leading to a not ideal utilization of the filter. (For interpretation of the references to colour in this figure legend, the reader is referred to the web version of this article.)

time and hence they get trapped (trajectory (b)). Particles can be trapped on other particles as indicated by the circle because of the electrical field inhomogeneity which is induced by the dielectric nanocapsules. Fig. 11B shows the resuspension mechanisms during backwashing with the electrical field turned off. Particles in area (a) will be easily resuspended because the gravitational body force points away from the surface and the movement induced by the hydrodynamic forces is not confined by the structure. Particles which are trapped on other particles as those in area (b) will be directly resuspended as they experience repelling electrostatic forces because of the like charges on the capsules. Most of the particles in area (c) cannot be resuspended as the gravitational body force is pointing towards the structure and the movement induced by hydrodynamic forces is constrained by the solid filter material and they must be lifted in order to resuspend.

3.3. Influence of module design

The design of both filtration modules, the small and the big one (cf. Section 2) was rather simplistic to assure easy observance of the process and simple filter changing and not to guarantee an optimal flow through the filter. This in turn implicates that the distribution of fluid inside the module is not optimal. A little slit has been left between the top electrode and the filter so that the fluid could equally distribute across the filter before crossing it. Nevertheless, inspection of the filter after the experiments suggests that most of the active filtration area is located close to the inlet (cf. Fig. 12). The colored areas indicate the parts of the filter in which most of the particles have been separated. Although inlet and outlet are located at diametrical points in the module, the flow distribution is uneven. Future experiments require a rather deliberated module design in the light of fluid input and output. Furthermore, a deeper understanding of the structure and material influence of the filter on the electric field disturbance is required for an optimized choice of filter and particle separation.

4. Conclusion

To conclude, we present a novel method to separate submicron particles, that experience a positive DEP effect in their solution by using a DEP driven deep-bed filtration. The filtration effect might be easily turned off by removing the superimposed electric field which is giving rise to the possibility to easily and safely resuspend the trapped nanocapsules. This we demonstrated by separating charged LbL nanocapsules from polyelectrolyte solution with identically charged side groups. Filters with a pore size more than two orders of magnitude larger ($d_{pore} = 20–130\ \mu$m) than the particle diameter ($d_p = 340$ nm) are used. Separation efficiencies without any superimposed electric field lie in the range between 0% and 8%. With the electric field turned on they reach 36% with ideal flow ($q = 11.11$ mL h^{-1} m^{-2}, membrane thickness $h = 2$ mm and pore

sizes $d = 20$–60 µm) and electric field parameters ($U = 200$ V and $f = 210$ kHz). A parametric study revealed that the separation efficiency is increasing with electric field strength, filter thickness, decreasing filter pore size and decreasing volume flow. In a semi-continuous test-run with several separation and backwashing steps we could achieve separation and recovery efficiencies of around 65%—which is a remarkable result when keeping in mind that neither the filter nor the module has been optimized. The successful separation of nanocapsules needed in molecular diagnostics demonstrates the high potential of the new technique for biotechnology. Further its ease makes this switchable filtration process attractive for nanoparticle separation and purification in general. In addition, these findings make the approach promising for a preparative DEP chromatography of nanoparticles.

As shown, in the current setup, a loss of nanocapsules is always occurring as a fraction of particles cannot be recovered during backwashing. To increase the absolute amount of recovered nano-particles, the separation efficiency has to be increased. This shall be achieved in the future by the establishment of a multi-stage cascade process with a parallel installment of separation stages to increase the overall flux through the setup.

Furthermore, numerical simulation of the electric field inside the porous structure and the influence of the pore structure and the filter material on the DEP velocity of the particles shall be investigated.

Acknowledgement

References

[1] B.G. De Geest, S. De Koker, G.B. Sukhorukov, O. Kreft, W.J. Parak, A.G. Skirtach, J. Demeester, S.C.D. Smedt, W.E. Hennink, Soft Matter (5) (2009) 282–291.
[2] E. Donath, G.B. Sukhorukov, F. Caruso, S.A. Davis, H. Möhwald, Angew. Chem. Int. Ed. 37 (1998) 2201–2205.
[3] G.B. Sukhorukov, H. Möhwald, Trends Biotechnol. 25 (2007) 93–98.
[4] G.B. Sukhorukov, A.L. Rogach, B. Zebli, T. Liedl, A.G. Skirtach, K. Köhler, A.A. Antipov, N. Gaponik, A.S. Susha, M. Winterhalter, W.J. Parak, Small 1 (2005) 194–200.
[5] C.S. Peyratout, L. Dähne, Angew. Chem. Int. Ed. 43 (2004) 3762–3783.
[6] E.M. Shchukina, D.G. Shchukin, Adv. Drug Deliver. Rev. 63 (2011) 837–846.
[7] M. Delcea, H. Möhwald, A.G. Skritach, Adv. Drug Deliver. Rev. 63 (2011) 730–747.
[8] K. Sato, K. Yoshida, S. Takahashi, J.i. Anzai, Adv. Drug. Deliver. Rev 63 (2011) 809–821.
[9] G. Ibarz, L. Dähne, E. Donath, H. Möhwald, Adv. Mater. 13 (2001) 1324–1327.
[10] G. Decher, Science 277 (1997) 1232–1237.
[11] G.B. Sukhorukov, E. Donath, H. Lichtenfeld, E. Knippel, M. Knippel, A. Budde, H. Möhwald, Colloid. Surface A 137 (1998) 253–266.
[12] A. Voigt, H. Lichtenfeld, G.B. Sukhorukov, H. Zastrow, E. Donath, H. Bäumler, H. Möhwald, Ind. Eng. Chem. Res. 38 (1999) 4037–4043.
[13] C. Kantak, S. Beyer, L. Yobas, T. Bansal, D. Trau, Lab Chip 11 (2011) 1030–1035.
[14] T. Weigert, J. Altmann, S. Ripperger, J. Membr. Sci. 159 (1999) 253–262.
[15] H.M. Huotari, I.H. Huisman, G. Trägårdh, J. Membr. Sci. 156 (1999) 49–60.
[16] T.Y. Chiu, F.J.G. Garcia, Sep. Purif. Technol. 78 (2011) 62–68.
[17] H.M. Huotari, G. Trägårdh, I.H. Huisman, Chem. Eng. Res. Des. 77 (1999) 461–468.
[18] A. Holder, J. Weik, J. Hinrichs, J. Membr. Sci. 446 (2013) 440–448.
[19] W.R. Bowen, A.L. Ahmad, AIChE J. 43 (1997) 959–970.
[20] R. Hofmann, T. Käppler, C. Posten, Sep. Purif. Technol. 51 (2006) 303–309.
[21] M. Loginov, M. Citeau, N. Lebovka, E. Vorobiev, Sep. Purif. Technol. 104 (2013) 89–99.
[22] C.-J. Chuang, C.-Y. Wu, C.-C. Wu, Desalination 223 (2008) 295–302.
[23] W.R. Bowen, R.A. Clark, J. Colloid Interface Sci. 97 (1984) 401–409.
[24] W.R. Bowen, H.A.M. Sabuni, Ind. Eng. Chem. Res 33 (1994) 1245–1249.
[25] F. Du, A. Hawari, M. Baune, J. Thöming, J. Membr. Sci. 336 (2009) 71–78.
[26] F. Du, P. Ciaciuch, S. Bohlen, Y. Wang, M. Baune, J. Thöming, J. Membr. Sci. 448 (2013) 256–261.
[27] S.H. Molla, S. Bhattacharjee, J. Membr. Sci. 255 (2005) 187–199.
[28] S.H. Molla, J.H. Maslivah, S. Bhattachariee, J. Colloid Interface Sci. 287 (2005) 338–350.
[29] S. Molla, S. Bhattacharjee, Langmuir 23 (2007) 10618–10627.
[30] E.B. Cummings, A.K. Singh, Anal. Chem. 75 (2003) 4724–4731.
[31] V. Chaurey, C. Polanco, C.-F. Chou, N.S. Swami, Biomicrofluidics 6 (2012) 012806.
[32] J.L. Baylon-Cardiel, B.H. Lapizco-Encinas, C. Reyes-Betanzo, A.V. Chavez-Santoscoy, S.O. Martinez-Chapa, Lab. Chip 9 (2009) 2896–2901.
[33] W.A. Braff, A. Pignier, C.R. Buie, Lab. Chip 12 (2012) 1327–1331.
[34] Y.-K. Cho, S. Kim, K. Lee, C. Park, J. Lee, C. Ko, Electrophoresis 30 (2009) 3153–3159.
[35] C. Illiescu, G. Xu, F.C. Loe, P.L. Ong, F.E.H. Tay, Electrophoresis 28 (2007) 1107–1114.
[36] H.A. Pohl, Dielectrophoresis, Cambridge University Press, Cambridge, 1978.
[37] H. Morgan, N.G. Green, AC Electrokinetics: Colloids and Nanoparticles, Research Studies Press Ltd., Baldock, 2003.
[38] F. Du, M. Baune, A. Kück, J. Thöming, Sep. Sci. Technol. 15 (2008) 3842–3855.
[39] F. Du, M. Baune, J. Thöming, J. Electrostat. 65 (2007) 452–458.
[40] N.G. Green, H. Morgan, J. Phys. Chem. B 103 (1999) 41–50.
[41] M. Baune, F. Du, J. Thöming, in: P.J. Plath, E. Hass (Eds.), Vernetzte Wissenschaften, Logos Verlag Berlin GmbH, Berlin, 2008, pp. 47–64.
[42] R. Pethig, G.H. Markx, Trends Biotechnol. 15 (1997) 426–432.
[43] N.G. Green, H. Morgan, J.J. Milner, J. Biochem. Biophys. Methods 35 (1997) 89–102.
[44] J. Voldman, Annu. Rev. Biomed. Eng. 8 (2006) 425–454.
[45] A. Castellanos, A. Ramos, A. González, N.G. Green, H. Morgan, J. Phys. D: Appl. Phys. 36 (2003) 2584–2597.
[46] J. Suehiro, G. Zhou, M. Imamura, M. Hara, IEEE Trans. Indus. Appl. 39 (2003) 1514–1521.
[47] S.K. Srivastava, A. Gencoglu, A.R. Minerick, Anal. Bioanal. Chem. 399 (2011) 301–321.
[48] N. Swami, C.-F. Chou, V. Ramamurthy, V. Chaurey, Lab. Chip 9 (2009) 3212–3220.
[49] R. Pethig, Biomicrofluidics 4 (2010) 022811.
[50] A. Zangwill, Modern Electrodynamics, Cambridge University Press, Cambridge, New York, Melbourne, Madrid, Cape Town, Singapore, São Paulo, Delhi, Mexico City, 2013.
[51] Y. Wang, F. Du, M. Baune, J. Thöming, Microfluid Nanofluid (2014), http://dx.doi.org/10.1007/s10404-013-1320-8.